Inhibited Hot-Carrier Cooling in $InAs/AlAs_{1-x}Sb_x$ Quantum Wells

H. Esmaielpour[1], V.R. Whiteside[1], H.P. Piyathilaka[2], S. Vijeyaragunathan[1], B. Wang[3], E. Adcock-Smith[4], K.P. Roberts[4], T.D. Mishima[1], M.B. Santos[1+], A.D. Bristow[2], and I.R. Sellers[1]

[1] *Department of Physics & Astronomy, University of Oklahoma, Norman, OK 73019*
[2] *Department of Physics & Astronomy, West Virginia University, Morgantown, WV 26501*
[3] *School of Chemical, Biological and Materials Engineering, University of Oklahoma, Norman, OK 73019*
[4] *Department of Chemistry and Biochemistry, University of Tulsa, Tulsa, OK 74104*

Semiconductor quantum wells (QWs) have been shown to exhibit decreased hot-carrier thermalization relative to bulk systems. Recently, we proposed that type-II QWs have the potential to further inhibit hot-carrier relaxation via the decoupling of the phonon channels through the spatial separation of photogenerated carriers. The spatial separation increases the radiative lifetime for the hot electrons, and leads to the formation of a robust phonon bottleneck at elevated temperatures [1,2]. A decoupling of the thermalization coefficient was observed when the system transitioned from efficient type-I radiative recombination at low temperature to less efficient type-II recombination at elevated temperatures.

The multiple-QW structure consists of a 10 nm $AlAs_{0.14}Sb_{0.86}$ barrier followed by 30 repetitions of a 2.4 nm InAs QW and a 10 nm $AlAs_{0.14}Sb_{0.86}$ barrier grown by molecular beam epitaxy on a GaAs (001) substrate. Photoluminescence (PL) measurements at several lattice temperatures T_L were modeled via a generalized Planck radiation law using the carrier temperature T_C as a fitting parameter. The effective temperature of the carriers above the lattice temperature ($\Delta T_C = T_C - T_L$) is weakly dependent on the excitation power, but becomes significantly hotter with increasing lattice temperature. When the lattice is at room temperature, the carrier temperature is 490K. Carrier lifetimes were determined by THz time-domain spectroscopy, which measures the AC photocurrent as a function of delay time between a near-infrared pump pulse and a THz probe pulse. Inspection of the three decay contributions reveals that the mechanism for the fast component (~0.01 ns) is different than for the intermediate and slow components. The fast decay is attributed to direct recombination within the QW, due to transitions from the electron ground state to localized hole states arising from alloy fluctuations. The intermediate (~0.3 ns) and slow (~2 ns) decay times, which dominate at high temperatures, are due to a two-step decay process between the same sets of initial and final states. These competing faster and slower components are attributed to the redistribution of photogenerated holes and the degeneracy of the valence band at elevated temperatures. This leads to competition and the convolution of the PL from multiple confined hole states and the ground state electrons. Confirmation of the long-lived nature of the photogenerated electrons in the InAs QWs supports the notion that the carriers in the QW facilitate a phonon bottleneck.

[1] J. Tang et al., *Appl. Phys. Lett.* **106**, 061902 (2015).
[2] H. Esmaielpour et al., *Progress in Photovoltaics: Research and Applications* **24**, 591 (2016).
[+] Author for correspondence: msantos@ou.edu

Supplementary Pages

Figure 1 shows the geometry for the THz measurements and schematic band-edge profiles for the processes that dominate at different temperatures. Figure 2 shows PL data and the extracted hot-carrier temperatures. Figure 3 shows the carrier dynamics as determined from the THz measurements.

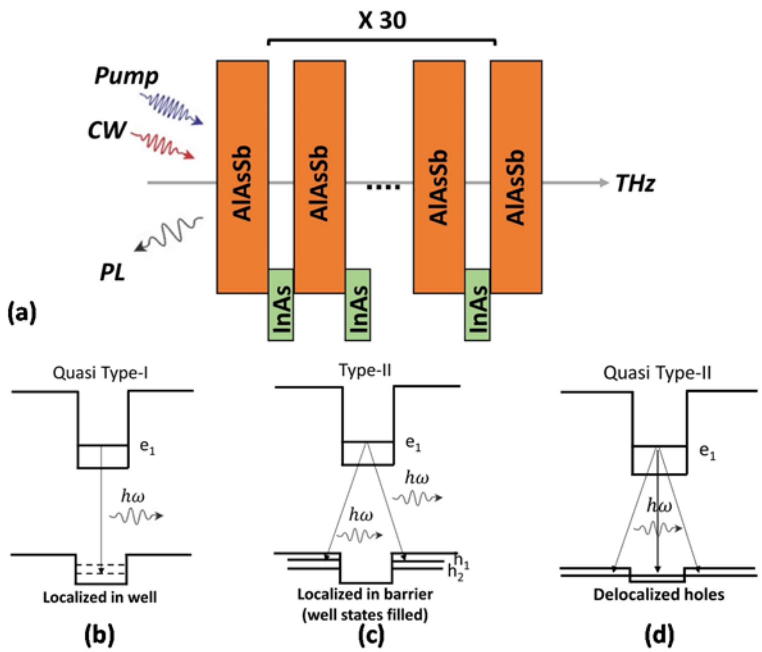

Figure 1: (a) Schematic of the experimental geometry, illustrating the orientation of the pulsed pump and THz probe, and the CW excitation and PL emission of the 30 InAs/AlAsSb multiple QW structure. (b) Quasi-type-I recombination at T < 100 K, dominated by quasi-direct transitions between holes localized in alloy fluctuations and electrons in the QWs. (c) The pure type-II transitions between electrons in the QW and holes in the barrier. (d) The quasi-type-II situation in which the hole states are degenerate and delocalized at high temperatures.

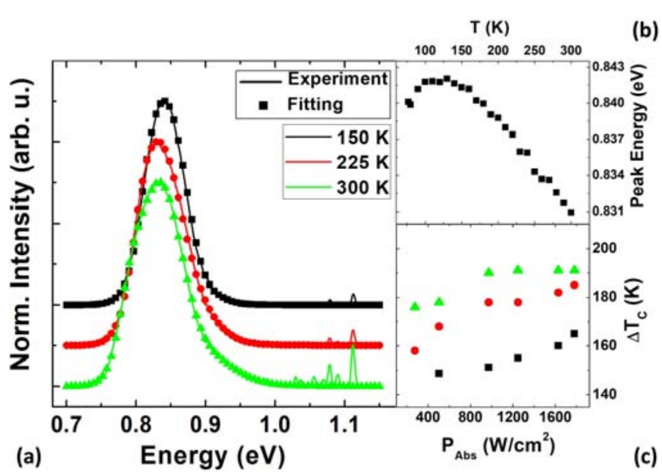

Figure 2: (a) Normalized temperature-dependent photoluminescence from 77 K to 300 K. (b) The peak energy as a function of temperature. (c) Extracted carrier temperature difference (ΔT_C) as a function of absorbed power at 150 K (black squares), 225 K (red circles), and 300 K (green triangles).

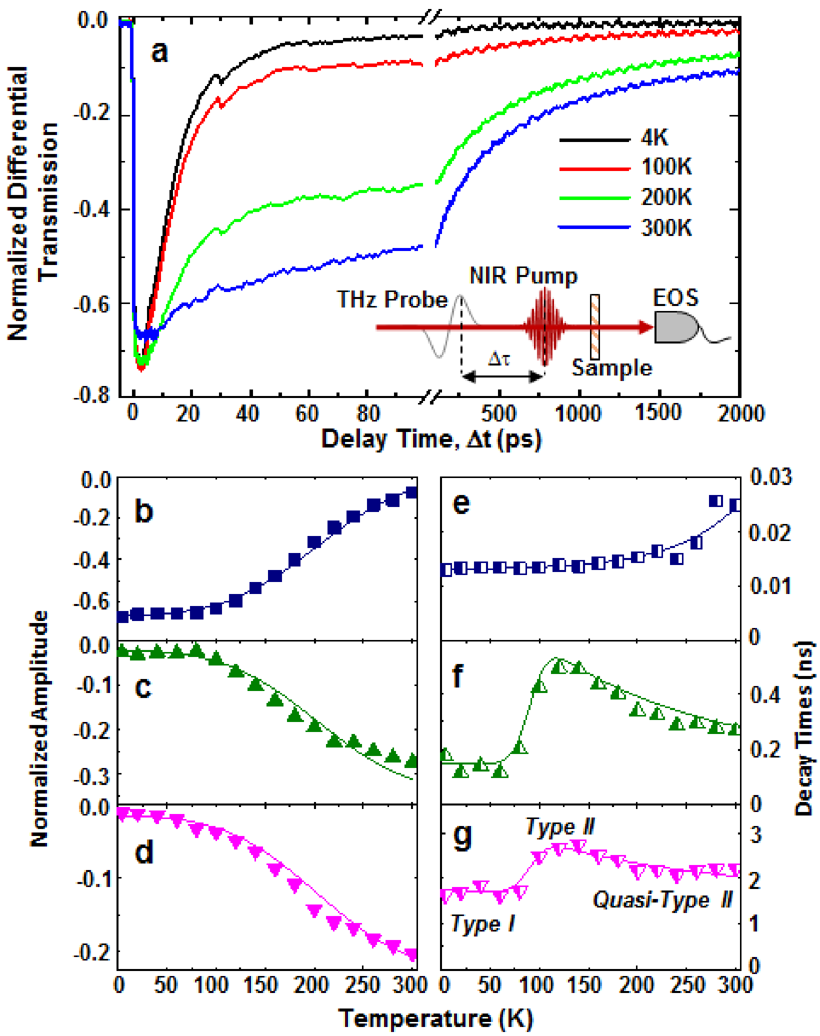

Figure 3: Carrier dynamics of the multiple QW system: (a) Normalized differential THz transmission for a range of lattice temperatures. The inset shows the collinear experimental geometry of the THz probe and near-infrared (NIR) pump. (b) – (d) and (e) – (g) are the amplitude and decay times of the fast, intermediate, and slow carrier dynamics extracted from fitting the transients. In (g), the regions of type-I, type-II and quasi-type II behavior are labeled.